Supplemental Figure 1

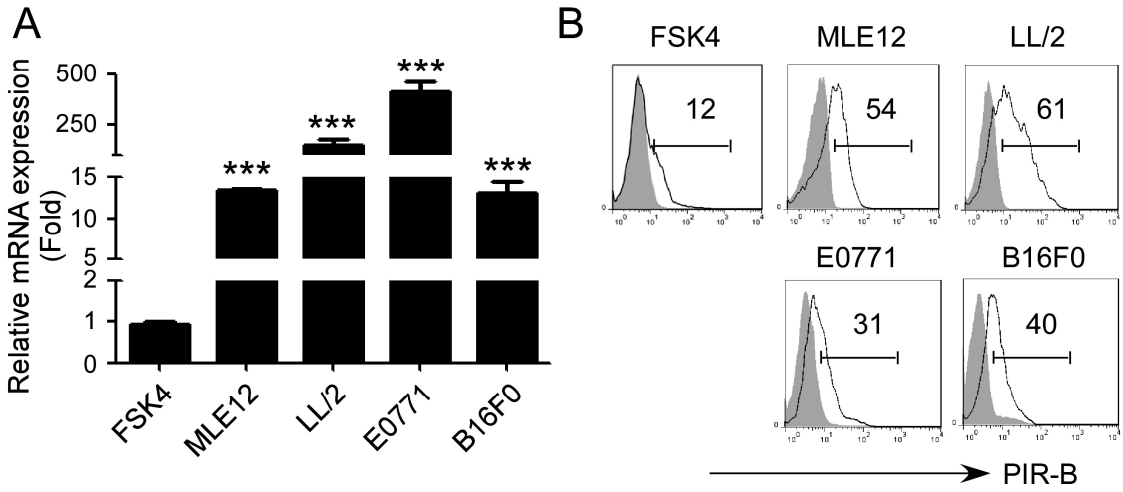

Supplemental Figure 1. Upregulated PIR-B expression in mouse tumor cells.

(A) and **(B)** Gene and protein expression levels of PIR-B were up-regulated in different mouse cancer cell lines using real-time qPCR and flow cytometry analyses. Tumor cell lines include lung cancer (MLE12, LL/2), breast cancer (E0771) and melanoma (B16F0) cell lines. The normal mammary gland endothelial cell line (FSK4) was included as a control. mRNA levels in each cell line were normalized to the relative quantity of β-actin expression and then adjusted to PIR-B levels in FSK4 cells (served as 1). Results shown in the histogram are mean ± SD from three independent experiments. ***P<0.001, compared with FSK4 cells (in A). Protein levels in cell lines were determined using the flow cytometry analyses (in B).

Supplemental Figure 2

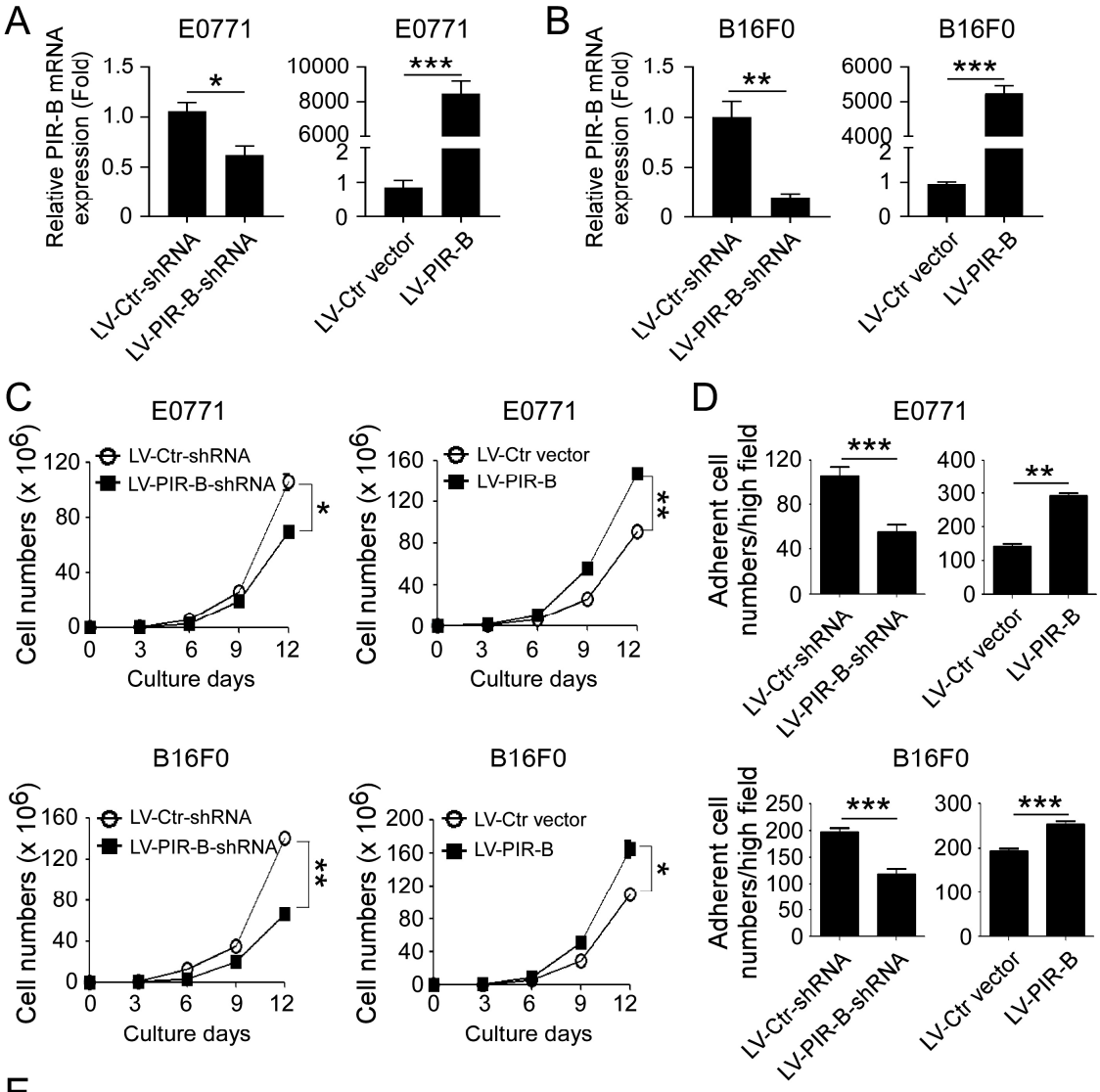

Supplemental Figure 2. PIR-B expression in tumor cells promotes their malignant behaviors.

(A) and **(B)** Knockdown and over-expression of PIR-B in E0771 (in A) and B16F0 (in B) tumor cells. Tumor cells were infected with lentivirus carrying PIR-B-shRNA or control shRNA, PIR-B or control vector at the MOI of 20 for 48 hours and then mRNA expression of PIR-B was analyzed by real-time qPCR. The expression levels of PIR-B gene were normalized to β-actin and adjusted to the levels in respective control virus-infected cells. Results shown are mean ± SD from three independent experiments. *P<0.05 and ***P<0.001.

(C) Knockdown of PIR-B expression significantly inhibited E0771 and B16F0 cell growth. However, over-expression of PIR-B promoted E0771 and B16F0 cell growth. Tumor cells were infected with lentivirus carrying PIR-B-shRNA, control shRNA, PIR-B or control vector at the MOI of 20 for 48 hours and then cultured at a starting number of 1×10^5/well in 6-well plates. Cell growth was evaluated by counting cell numbers at different time points. *P<0.05 and **P<0.01.

(D) Knockdown of PIR-B expression in E0771 and B16F0 cells markedly decreased the adhesive capacity of tumor cells. In contrast, over-expression of PIR-B promoted E0771 and B16F0 cell adhesive capacity. Cell preparation was identical to (C). 1×10^5 tumor cells were seeded in fibronectin pre-coated 96-well plates. After incubation at 37 °C for 45 minutes, the adherent tumor cells on the plates were fixed and stained with 0.03% crystal violet. Adherent tumor cells were counted and averaged in 10 fields at high magnification (× 400). **P<0.01 and ***P<0.001.

(E) Knockdown of PIR-B expression in E0771 and B16F0 cells dramatically decreased the migration of tumor cells in the wound closure assays. In contrast, over-expression of PIR-B enhanced E0771 and B16F0 cell migration ability. Cell preparation was identical to (C). 4×10^5 tumor cells were plated into 6-well plates. After 24 hours of culture, the scratches were made and photographed at 0 and 12 hours of culture.

Supplemental Figure 3

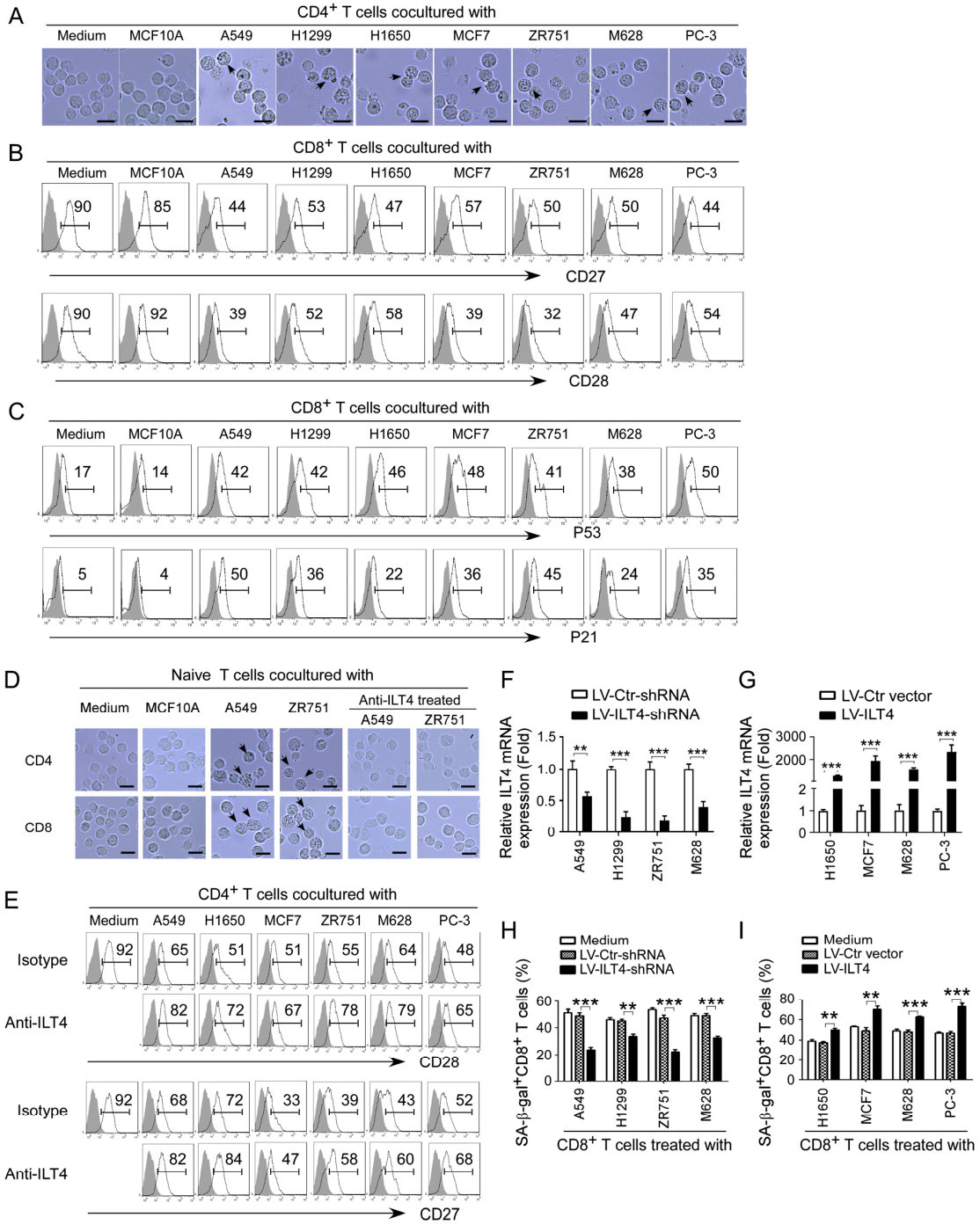

Supplemental Figure 3. Tumor-derived ILT4 induces T-cell senescence

(A) Co-culture with different tumor cells significantly increased SA-β-Gal$^+$ T cell populations in co-cultured CD4$^+$ T cells. However, T cells co-cultured with the breast epithelial cell line MCF10A had no or little SA-β-Gal expression. Cell treatment and culture procedure were the same as in Figure 2A. SA-β-Gal positive cells were indicated as dark blue granules in the cytoplasm. Tumor cell lines included NSCLC (A549, H1299 and H1650), breast cancer (MCF7 and ZR751), melanoma (M628) and prostate cancer (PC-3).

(B) and **(C)** Tumor cell treatment decreased expression of co-stimulatory molecules CD27 and CD28 (in B) but upregulated expression of cell cycle regulatory molecules P53 and P21 (in C) in senescent CD8$^+$ T cells. Cell treatment and procedure were the same as in Figure 2A. Expression levels of CD27, CD28, P53, and P21 in co-cultured CD8$^+$ T cells were analyzed by the flow cytometry analyses.

(D) and **(E)** Blockade of ILT4 through an anti-ILT4 neutralizing antibody remarkably prevented tumor-induced senescence (in D) and loss of CD27 and CD28 expression (in E) in both CD4$^+$ and CD8$^+$ T cells. The cell co-culture procedures are identical to the description in Figure 2A. Anti-ILT4 neutralizing antibody (500 ng/ml) or isotype control antibody were included in the co-culture system. SA-β-Gal expression in T cells were determined and indicated (in D). Expression levels of CD27 and CD28, P53 and P21 in co-cultured T cells were analyzed by the flow cytometry analyses (in E).

(F) and **(G)** Knockdown or overexpression of ILT4 in tumor cells. Tumor cell lines (A549, H1299, ZR751 and M628) with ILT4 high expression were infected with lentivirus carrying ILT4 shRNA or control shRNA (in F), or tumor cell lines (H1650, MCF7, M628 and PC-3) were infected with lentivirus carrying ILT4 or control vector (in G), at the MOI of 5-10 for 48 hours and then mRNA expression of ILT4 was analyzed by real-time qPCR. The expression levels of ILT4 gene were normalized to β-actin and adjusted to the level in respective control virus-infected cells (served as 1). Results shown are mean ± SD from three independent experiments. **P<0.01 and ***P<0.001.

(H) Knockdown of ILT4 in tumor cells prevented T cell senescence induced by tumor cells. Tumor cell lines (A549, H1299, ZR751 and M628) with ILT4 high expression were infected with lentivirus carrying ILT4 shRNA or control shRNA at the MOI of 5-10 for 48 hours and then co-cultured with T cells as described in Figure 2. SA-β-Gal$^+$ cell populations in co-cultured CD8$^+$ T cells were determined. Results shown in the histogram are mean ± SD from three independent experiments. **P<0.01 and ***P<0.001, compared with the control LV-Ctr-shRNA group.

(I) Overexpression of ILT4 in tumor cells promoted T cell senescence induced by tumor cells. Tumor cell lines (H1650, MCF7, M628 and PC-3) were infected with lentivirus carrying ILT4 or control vector at the MOI of 5-10 for 48 hours and then co-cultured with T cells as described in Figure 2. SA-β-Gal$^+$ cell populations in co-cultured CD8$^+$ T cells were determined. Results shown in the histogram are mean ± SD from three independent experiments. **P<0.01 and ***P<0.001, compared with the control vector group.

Supplemental Figure 4

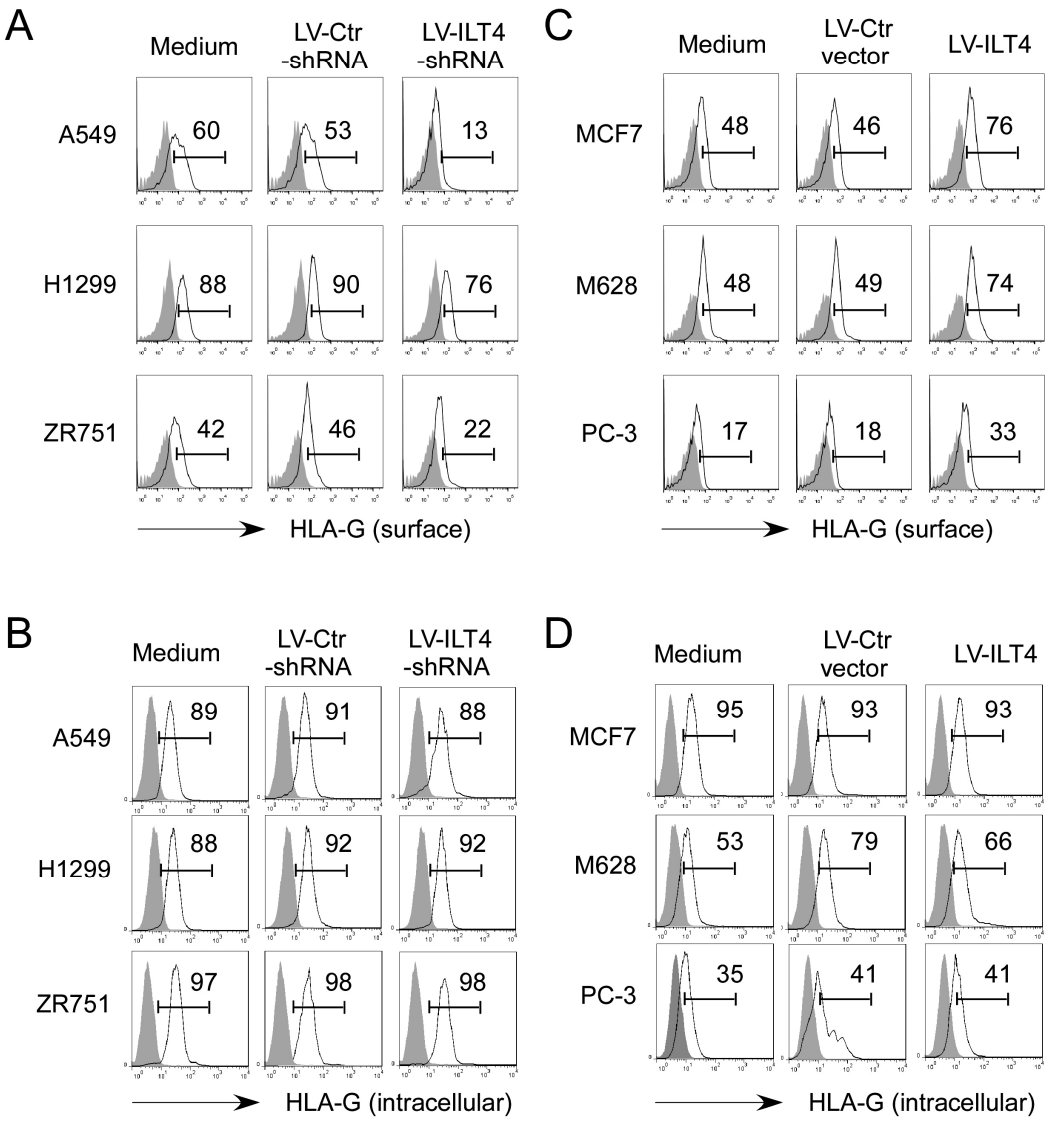

Supplemental Figure 4. Knockdown or overexpression of ILT4 in tumor cells affects HLA-G expression in tumor cells.

(A)-(D) A549, H1299 and ZR751 tumor cell lines were infected with lentivirus carrying ILT4 shRNA or control shRNA at the MOI of 5-10 for 72 hours (in A and B). Furthermore, MCF7, M628 and PC-3 tumor cells were infected with lentivirus carrying ILT4 or control vector at the MOI of 5-10 for 72 hours (in C and D). Surface (in A and C) and intracellular HLA-G expression (in B and D) in tumor cells was determined by the flow cytometry analyses.

Supplemental Figure 5

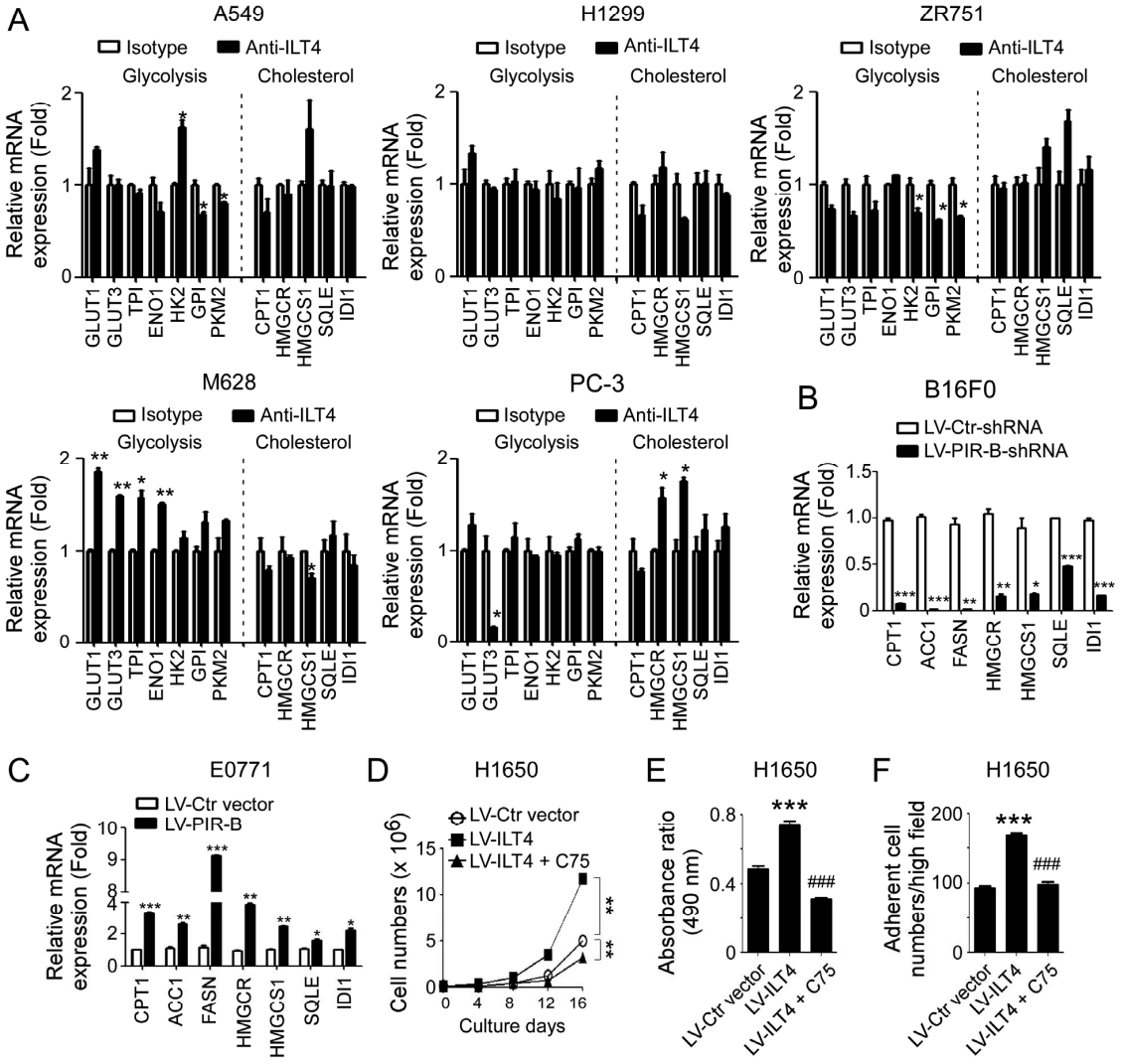

Supplemental Figure 5. ILT4-induced up-regulation of lipid metabolism in tumor cells promotes T cell senescence.

(A) Gene expression levels of key enzymes associated with glycolysis and cholesterol synthesis in tumor cells after neutralization of ILT4. Human tumor cell lines were treated with anti-ILT4 (500 ng/ml) neutralizing antibody or isotype control antibody for 48 hours, and mRNA expression levels of each enzyme were determined by real-time qPCR. The expression of each gene was normalized to β-actin and adjusted to the levels in corresponding isotype antibody treated cells (served as 1). Results shown in the histogram are mean ± SD from three independent experiments. *P<0.05 and **P<0.01, compared with the cells treated with isotype antibody.

(B) Knockdown of PIR-B in B16F0 tumor cells (PIR-B high expression) decreased gene expression levels of key enzymes for fatty acid oxidation (CPT1) and synthesis (ACC1 and FASN), and cholesterol synthesis (HMGCR, HMGCS1, SQLE and IDI1). B16F0 tumor cells were transfected with lentivirus-based PIR-B shRNA or control shRNA for 48 hours and then mRNA expression of each enzyme was analyzed by real-time qPCR. The expression levels of each gene were normalized to β-actin and adjusted to the level in respective control group (served as 1). Results shown in the histogram are mean ± SD from three independent experiments. *P<0.05, **P<0.01 and ***P<0.001, compared with the control shRNA (LV-Ctr-shRNA)-transfected cells.

(C) Overexpression of PIR-B in E0771 (low PIR-B expression) increased gene expression of key enzymes involved in fatty acid oxidation (CPT1) and synthesis (ACC1 and FASN), and cholesterol synthesis (HMGCR, HMGCS1, SQLE and IDI1). E0771 cells were transfected with lentivirus-based PIR-B or control vector for 24 hours, and mRNA expression of each enzyme was analyzed by real-time qPCR. The expression levels of each gene were normalized to β-actin and adjusted to the level in respective control group (served as 1). Results shown in the histogram are mean ± SD from three independent experiments. *P<0.05, **P<0.01 and ***P<0.001, compared with the control vector (LV-Ctr-vector)-transfected cells.

(D)-(F) Overexpression of ILT4 promoted H1650 cell proliferation and adhension, while addition of FASN inhibitor C75 in the culture system reversed those effects. H1650 cells were infected with lentivirus carrying LV-ILT4 or LV-control vector and then cultured in the presence or absence of FASN inhibitor C75 (5 μM). The cell numbers were counted every four days (in D). The MTT proliferation assay was performed at day 4 after lentivirus infection (in E). Cell adhesion assay were performed at day 3 after lentivirus infection (in F). Results shown are mean ± SD from three independent experiments. **P<0.01 and ***P<0.001, compared with the LV-Ctr vector group. $^{###}$P<0.001, compared with LV-ILT4 group.

Supplemental Table 1. Specific primers used in the study.

Gene	Primer (Forward)	Primer (Reverse)
Human		
ILT4	ACATCGACCCAGAGAAAGGCTGAT	TCCTTCACGGCAGCATAGAGGTTT
CPT1	ATCAATCGGACTCTGGAAACGG	TCAGGGAGTAGCGCATGGT
ACC1	TCACACCTGAAGACCTTAAAGCC	AGCCCACACTGCTTGTACTG
FASN	ACAGCGGGGAATGGGTACT	GACTGGTACAACGAGCGGAT
HMGCR	GTGAGATCTGGAGGATCCAAGG	GATGGGAGGCCACAAAGAGG
HMGCS1	GTTGGCGGCTATAAAGCTGGT	CCTTCGGGCACAAGCG
SQLE	TGACAATTCTCATCTGAGGTCCA	TCCCAAAAGAAGAACACCTCGT
IDI1	CGGAGGCTGATCAGTGTTCTA	TGTTGCTTGTCGAGGTGGTT
Glut1	AATGGCTCCGGTATCGTCAAC	GCTCAGATAGGACATCCAGGGTA
Glut3	GCTCTCTGGGATCAATGCTGTGT	CTTCCTGCCCTTTCCACCAGA
HK2	AACAGCCTGGACCAGAGCAT	GCCAACAATGAGGCCAACTT
Eno1	CGCCTTAGCTAGGCAGGAAG	GGTGAACTTCTAGCCACTGGG
TPI1	AGGCATGTCTTTGGGGAGTC	AGTCCTTCACGTTATCTGCGA
GPI	GATGGTAGCTCTCTGCAGCC	GCCATGGCGGGACTCTTG
PKM2	ACGAGAACATCCTGTGGCTG	AGGAAGTCGGCACCTTTCTG
GAPDH	AGCCGCATCTTCTTTTGCGTCG	GACCAGGCGCCCAATACG
β-actin	TGGCACCCAGCACAATGAA	CTAAGTCATAGTCCGCCTAGAAGCA
Mouse		
PIR-B	TCAGGAAAGATGTCCAGAAAGAGA	GCTGTTCAGCTCCACTCCAT
CPT1	AGATCAATCGGACCCTAGACAC	CAGCGAGTAGCGCATAGTCA
ACC1	AATGAACGTGCAATCCGATTTG	ACTCCACATTTGCGTAATTGTTG
FASN	GGCTCTATGGATTACCCAAGC	CCAGTGTTCGTTCCTCGGA
HMGCR	TCTTGTGGAATGCCTTGTGATT	GGGTTACGGGGTTTGGTTTAT
HMGCS1	AACTGGTGCAGAAATCTCTAGC	GGTTGAATAGCTCAGAACTAGCC
SQLE	GCTGGGCCTTGGAGATACAG	CAGTGGGTACGGAATTTGAACT
IDI1	CGAACCCTCCTCAAGAAGCC	CCTAGAACACAGAGATTCCGGC
GAPDH	ATGAAGGGGTCGTTGATGGC	GGGTTCCTATAAATACGGACTGC
β-actin	GATCAAGATCATTGCTCCTCCTG	AGGGTGTAAAACGCAGCTCA